A Look at Some Challenging Problems in Computational Electromagnetics

Raj Mittra

Electromagnetic Communication Lab, Department of Electrical Engineering
Pennsylvania State University
University Park, PA 16802-2705, USA
Tel: +1 (814) 865-1298; Fax: +1 (814) 865-1299; E-mail: rajmittra@ieee.org

Abstract

Recent years have seen a spectacular increase in our capability to model, simulate the performance of, and design complex electromagnetic systems. Much progress has been made in enhancing the available numerical techniques, viz., the Method of Moments (MoM), the Finite-Element Method (FEM), and the Finite-Difference Time-Domain (FDTD) or its variants. Great strides have recently been made in enlarging the scope of MoM via the use of the Fast Multipole Method (FMM), which has made it feasible for us to solve problems that require the handling of 106 degrees of freedom, or even higher, and distributed processing has enabled the FDTD to handle upward of 109 degrees of freedom on a moderate-size computing platform. Despite this recent progress, many practical computational electromagnetic (CEM) modeling problems of interest present formidable challenges, and the search for numerically efficient techniques to solve large problems involving complex structures continues unabated.

The objectives of this paper are to identify some of these challenging problems encountered by the author during the last five years, and to present the results of application of a technique called CBFM – developed at the EMC Laboratory at Penn State – that has been found useful for addressing them.

Keywords: Electromagnetic analysis; electromagnetic scattering; antenna arrays; frequency selective surfaces; electromagnetic compatibility; electromagnetic interference

1. Introduction

Recent years have seen a spectacular increase in our capability to model, simulate the performance of, and design complex electromagnetic systems. Much progress has been made in enhancing the available numerical techniques, viz., the Method of Moments (MoM), the Finite-Element Method (FEM), and the Finite-Difference Time-Domain (FDTD) or its variants. Of these, the MoM is best suited for perfect electrically conducting (PEC) structures or those with homogeneous dielectric coatings. The finite methods can handle arbitrary objects, comprised of both PECs and inhomogeneous dielectrics – albeit at a computational cost that is higher than that of the MoM for PEC objects. Since the MoM generates a dense matrix, typically the number of degrees of freedom that it can handle is usually smaller than can be dealt with using the FEM or the FDTD. Great strides have recently been made in enlarging the scope of the MoM via the use of the Fast Multipole Method (FMM), which has made it feasible for us to solve problems that require the handling of 10^6 degrees of freedom or even higher. The Fast Multipole Method accomplishes this by bypassing the generation (and inversion) of the full matrix, storing only the near-field interaction terms, and performing the matrix-vector products required in the iterative solution by using the multipole method. In contrast, the FDTD can routinely handle 10^9 degrees of freedom on a moderate-size computing platform, but it requires a discretization that is two to three times finer than that employed in the MoM. Furthermore, it deals with all six components of the E and H fields, as opposed to just two components of the surface currents employed in the MoM formulation. Hence, the MoM techniques are almost always preferred whenever they can be used for the problem at hand.

At this point, it may be worth noting an important distinction between the FDTD and the FEM. Though the FEM only generates a sparse matrix, the boundary-element truncation of the FEM adds a dense matrix component to it, the characteristics of which closely resemble those of the MoM matrix. Consequently, some of the storage and other advantages related to solution strategies of such matrices are compromised when the Boundary Element Method (BEM) – rather than the perfectly matched layer (PML) – is employed for the truncation of the computational boundary in the FEM. Our experience shows that in contrast to the FEM, the FDTD is not plagued with ill-conditioning and related problems when it uses the perfectly matched layer for mesh truncation, and this type of truncation introduces little change in the FDTD solution algorithm However, unless designed appropriately, the perfectly matched layer can introduce instabilities in the FDTD algorithm, especially if the perfectly matched layer boundary is too close to the object.

Before closing this section, we mention that the FDTD algorithm is embarrassingly parallel, and this may provide it an important edge over the MoM (as well as the FEM/BEM) when solving

large problems on parallel or distributed-processing platforms. Nonetheless, the FEM and MoM have their own unique advantages for solving a class of problems, and some codes based on these algorithms have also been parallelized using specialized schemes.

Finally, we would be remiss if we did not point out that asymptotic methods, such as the Geometrical Theory of Diffraction (GTD) or the Physical Theory of Diffraction (PTD), are probably the only viable approaches currently available for solving a class of very large problems, the sizes of which exceed the handling capacities of the MoM, the FEM, or the FDTD. However, these methods are often limited in their application to PEC structures, or to those with surfaces that can be described in terms of approximate reflection coefficients. Many practical CEM modeling problems of interest today do not fall into this category and, hence, the search for numerically efficient rigorous techniques, as well as for hybrid algorithms for solving large problems involving complex structures, continues unabated.

2. Challenging Problems in CEM

Although we have presented a brief survey of CEM techniques in the last section, our focus in this paper is not to delve deeply into the subject, but to describe a number of complex EM modeling problems of great practical interest that severely task the available CEM tools. We will now describe a number of these problems in this section.

2.1 Large Planar Arrays

Figures 1 through 3 show three different representative planar arrays the elements of which are rectangular waveguides, probe-fed microstrip patches, and Vivaldi patches, respectively, the latter being useful for broadband applications. Except for the waveguide element, which is PEC, it is preferable – if not necessary – to use either the FEM or the FDTD to handle the above problems because of the finite nature of the dielectric substrate.

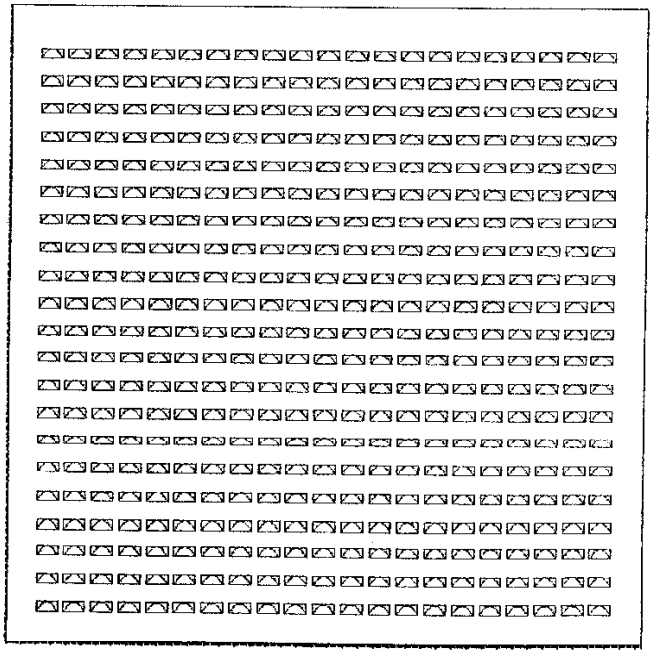

Figure 1. A rectangular waveguide array.

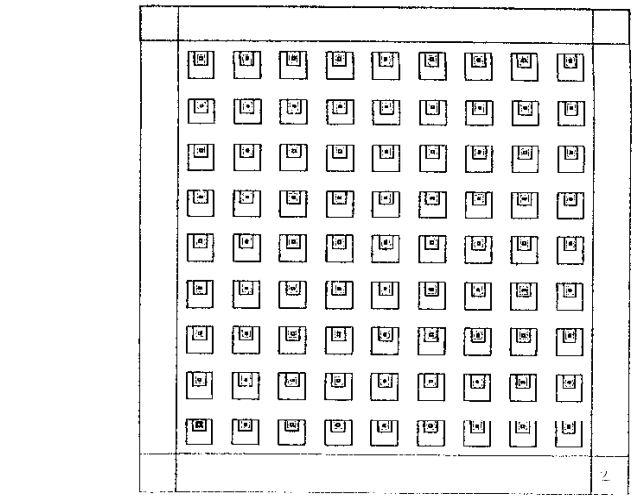

Figure 2. A probe-fed microstrip-patch array.

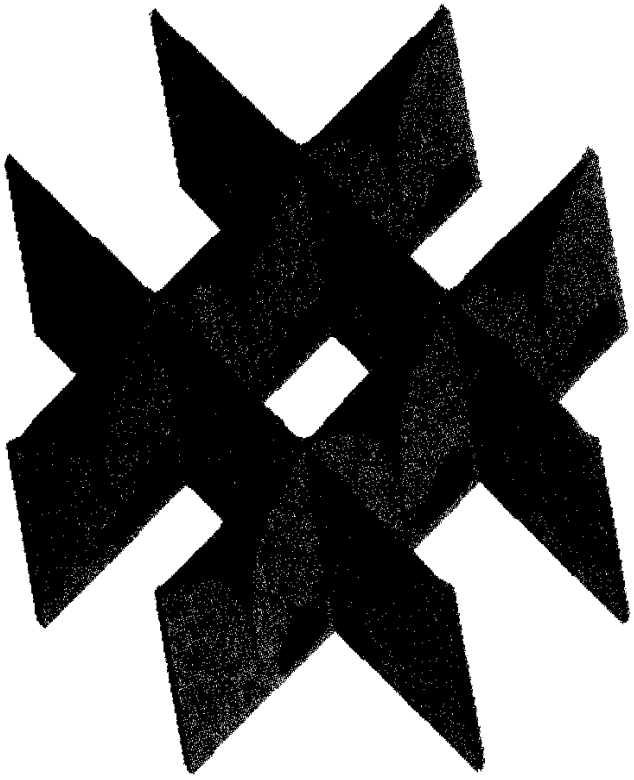

Figure 3. A dual-polarized Vivaldi array.

Accurate modeling of the feed region of the microstrip patch of the Vivaldi – which is necessary for reliable prediction of the input impedance of the array – requires us to use a fine discretization, on the order $\lambda/100$ or less. This, in turn, severely burdens the memory, and it may be necessary to use as much as 1 GB of RAM per element for such a Vivaldi element, although the RAM requirements are smaller for the patch and the waveguide elements. Obviously, the memory problem is exacerbated when the

elements are arrayed, as they are in practice to form a phased array comprising hundreds if not tens of thousands of elements, often used in radar and communication applications. Such large array problems indeed pose a formidable challenge, especially when the designer of the array demands that the solution be generated in a reasonable time: taking at most a few hours of CPU time, for instance.

None of the existing CEM codes are up to this challenge, and it has prompted the code developers to take a fresh look at the above problem. We will later mention one of these approaches, called the Characteristic Basis Function Method (CBFM) [1-4]. When combined with the Windowed Plane Wave Spectrum (WPWS) approach [5, 6], this can not only handle the large array problem, but several others we are going to describe in this section. Several other excellent and innovative and approaches have also been introduced recently by Kindt and Volakis [7], Capolino et al. [8], Prinoli and her colleagues [9], and Maci et al. [10], among others.

2.2 Frequency-Selective-Surface (FSS) Radomes

FSSs find extensive applications as high-performance radomes because of their frequency-selective characteristics, which enable the desired radiation from the antenna to pass through the radome cover but block the interfering signals from interrogating radars operating at out-of-band frequencies. A few typical FSS elements – which can either be of a patch or an aperture type (low- or high-pass) – are shown in Figure 4a. The metallization of these elements can in general have a non-infinitesimal thickness, which may make the problem difficult to handle using the MoM in an efficient manner.

The FSSs are usually analyzed under the assumption that they are planar, doubly-periodic, infinite structures. This, in turn, enables one to reduce the problem to a single unit cell, with dimensions that are only on the order of one wavelength. Even so, depending on the fineness of the geometry and the complexity of its shape, it may be necessary to discretize the element using 1024 × 1024 pixels, resulting in a large number of unknowns if the metalization fills the bulk of the unit cell. Nonetheless, there are a number of MoM-based FSS simulation codes that can handle arbitrarily-shaped "thin" FSS elements in a reasonably efficient manner. For thick elements, one can use either FEM- or FDTD-based codes and, once again – since the size of the unit cell is only on the order of 1λ – the problem is manageable. This is true for multiple screens as well, for which the response can be obtained by using a cascading approach.

However, the problem size increases by many orders of magnitude when we attempt to analyze a finite FSS (see Figure 5), which is often hundreds of wavelengths in size. This is because the problem geometry is no longer periodic and, hence, reducible to a single unit cell for the purpose of analysis. An approximate approach that is frequently used is to assume that the current distribution in the truncated FSS is the same as that in the infinite structure and, of course, identically zero outside. However, such an approximation fails to capture the edge effects, including the excitation of surface waves, which can affect the scattering characteristics of the FSS in the far-end sidelobe regions. In addition, it is difficult to estimate the performance of the truncated FSS when it is mounted in a frame (as is often the case), where the frame can be either a PEC or a surface coated with an absorber.

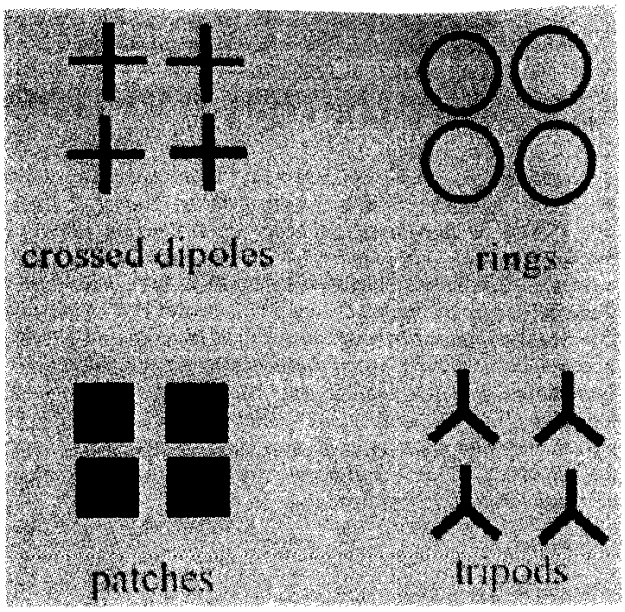

Figure 4a. Typical FSS elements.

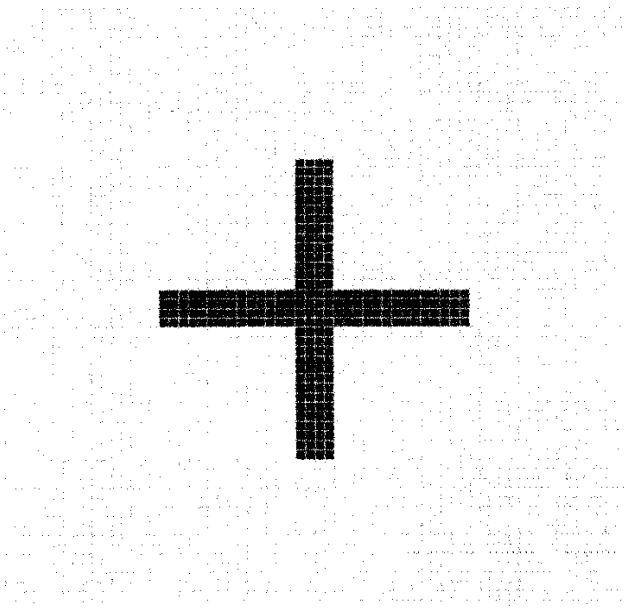

Figure 4b. A discretization of the unit cell of an FSS element.

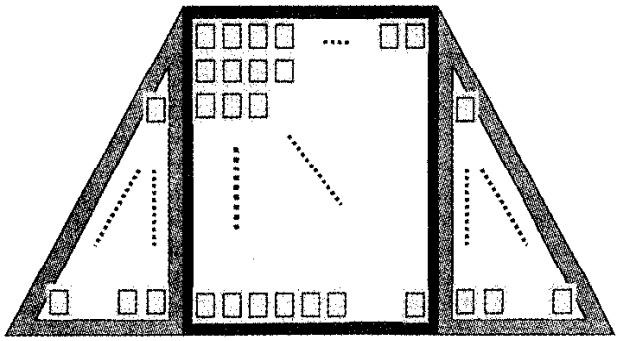

Figure 5. A trapezoidal-shaped finite FSS with a frame illuminated by a 21 × 21 element microstrip-patch array.

One approach to addressing the truncated FSS problem, with or without the frame, has been introduced recently in [5], and is briefly described in Section 3. The Windowed Plane Wave Spectrum technique has been employed in this approach, which renders this seemingly untenable problem manageable.

2.3 FSS Radomes Comprised of Multiple Screens with Non-Commensurate Periodicities

Often, a single FSS screen is not adequate for realizing the frequency response we desire for the radome, and this prompts us to use multiple screens to realize a greater degree of design flexibility (see Figure 6). Sometimes, to achieve a wider bandwidth or a sharper falloff of the response, the periodicities of the different screens may be chosen to be dissimilar as well as non-commensurate. The periodic characteristics of the FSS are spoiled for such screen composites, and, without the benefit of this feature, the problem of analyzing such composites becomes totally untenable, even when the individual screens are assumed to be infinite and doubly-periodic. It is therefore not surprising that this problem remained unsolved until very recently, except for the somewhat trivial case of widely separated screens with no interaction between them, except via the fundamental Floquet harmonic [11].

A new approach to handling this problem has recently been proposed, and it is now possible to analyze the general FSS composites in a numerically efficient manner. For details, the reader is referred to [12].

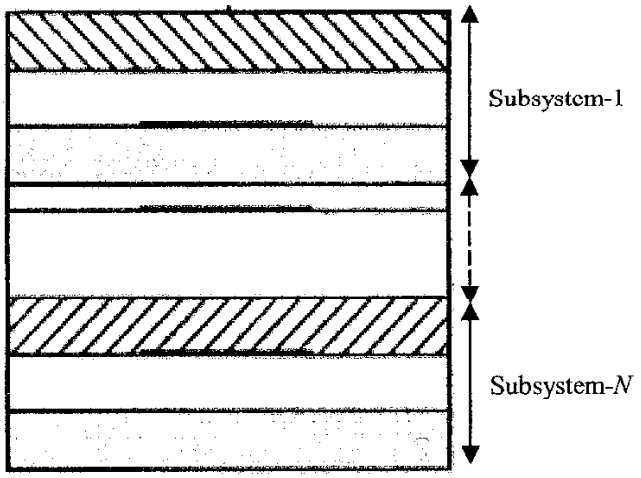

Figure 6. A composite structure consisting of N stacked subsystems comprised of dielectric layers and FSS screens.

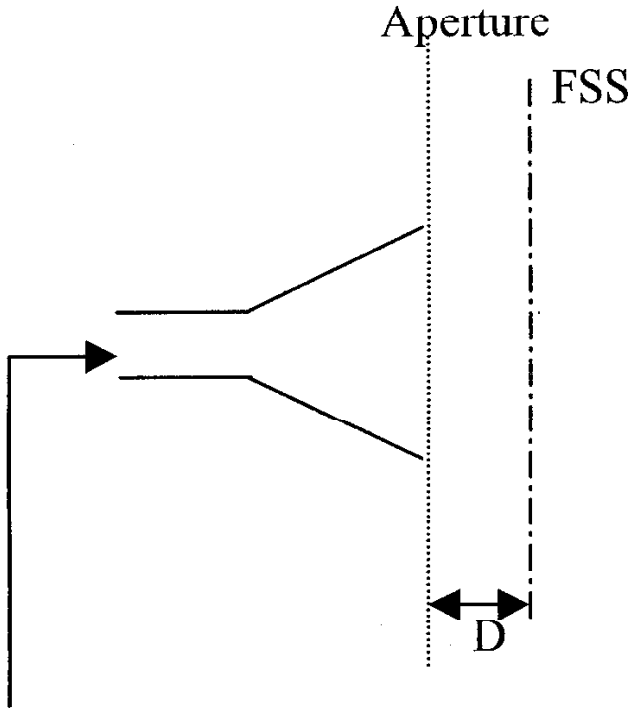

Figure 7. A Ku-band pyramidal horn covered with an FSS radome, with $D = 30$ cm, operating at 30.5 GHz.

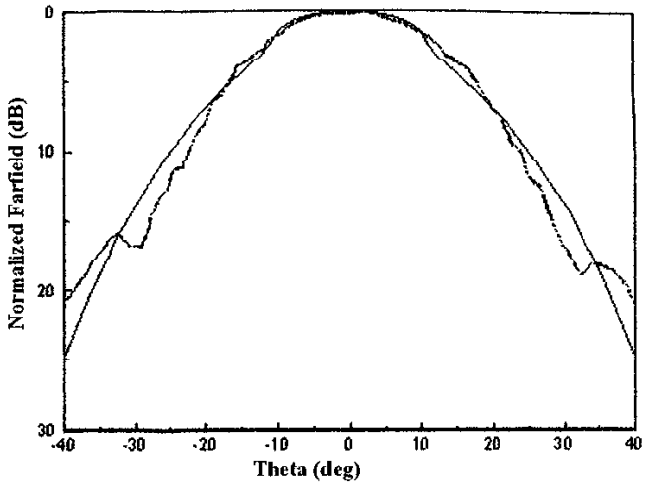

Figure 8. The far-field pattern of the horn antenna alone, computed from the FDTD aperture field: FDTD solution (solid line) and measured data (dashed line).

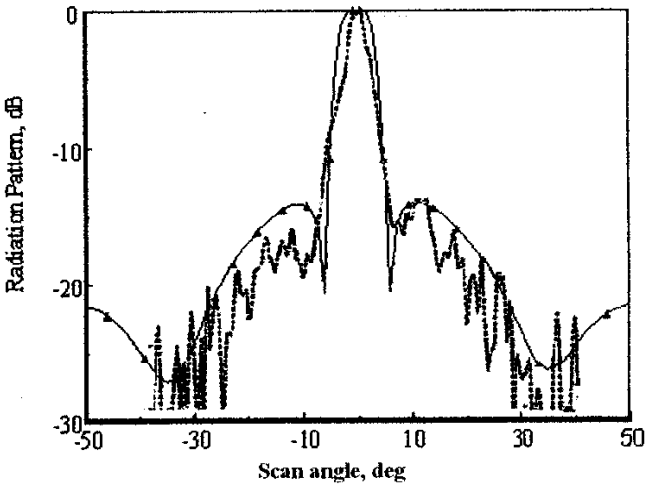

Figure 9. The far-field of the horn in the presence of the FSS radome at 30.5 GHz: measured data (dashed line) and present approach (triangles).

2.4 FSS Radome Located in Proximity of a Phased Array

More often than not, the FSS radome covering a phased array is located close to the array; furthermore, it is very unlikely for them to have the same periodicities. Yet, the presence of the radome can have a noticeable effect on the performance of the array, and it is often necessary to accurately assess this effect. We illustrate this via a simple example of a horn antenna operating close to an FSS radome, as shown in Figure 7. The far-field patterns of the antenna and antenna/FSS composite are shown in Figures 8 and 9, where some measured data are also included.

When the separation distance between the two is not too small, a perturbation approach [6] can be employed to predict the performance of the array/radome composite. This approach is practical when the first- and second-order effects adequately describe the antenna-radome interaction and the higher-order terms are negligible.

However, a more sophisticated approach is needed when the interaction between the two is strong, and one such approach has recently been introduced with encouraging results (see Section 3). The problem becomes much more difficult and computer-intensive when we are dealing with an array antenna covered by an FSS radome, as, for instance, shown in Figure 10. Before closing this section, we also mention the space-frame radomes that cover large reflector and phased-array antennas for protection from the weather. These radomes are comprised of dielectric membranes supported by metallic frames that are not periodic in nature. Such radomes are huge structures that have defied analysis except by methods based on relatively simple approximations, e.g., the Induced Field Ration (IFR) approach [13, 14]. A more accurate analysis of this challenging problem is very desirable in certain frequency ranges, usually in the lower end of the band.

2.5 Conformal Arrays

The design of large planar phased arrays – typically, doubly-periodic in the infinite limit – is greatly facilitated by first analyzing a single unit cell, and then using the array-factor (AF) approach to predict the performance of a truncated, finite array. As mentioned earlier, a more sophisticated approach is to use the Characteristic Basis Function Method (CBFM), which does not rely upon the approximation involved in the array-factor technique.

In many applications, an array designer does not enjoy the luxury of having a planar surface on which to place the array, and is asked to design a conformal version of the array on a doubly-curved surface, instead. Once the design of the array deviates from the planar limit, its periodic nature is spoiled, and, in common with the other cases we have discussed before, the array becomes a very difficult problem to analyze.

An example of such a problem is shown in Figure 11, where it is desired to design an array of circular patches on a spherical surface (or on one that is doubly-curved, in general) where the number of elements can run into the hundreds, if not thousands. Since the patches are typically placed on a dielectric substrate, the analysis of this type of conformal-array problem presents a formidable challenge, and not much has been written on this topic that provides us a clue as to how to handle this very difficult problem. The difficulty arises not only from the lack of periodicity, but also from the unavailability of a Green's function in a convenient form, especially for an arbitrarily curved surface. Recently, the CBFM has been successfully applied to this problem as well, and some representative results are presented in Section 3.

2.6 EMI/EMC Problems Associated with Antenna Placements on Complex Platforms

Very often, an antenna designer is asked where a new antenna should be placed on a complex platform so that the interference between it and the other antennas that are already located on the same platform would be minimized. Obviously, the designer needs a reliable tool to estimate the coupling between the two antennas. But the problem of modeling the system becomes a truly challenging one when the antennas in question happen to be large arrays (or reflectors that are tens of wavelengths in diameter) and they both share a complex platform such as an airplane, the top side of a ship, a tank, a helicopter, or a Humvee (HMMWV), which are many tens or even hundreds of wavelengths in size. An example of such a real-life coupling problem, the detailed dimensions of which are omitted here, is sketched in Figure 12.

We know from our previous discussion that a large phased-array problem is difficult to analyze. The analysis of large reflector problems, while manageable in the transmitting mode, become even more difficult when they are treated as scatterers illuminated by waves originating from the array antenna but arriving on a reflector either directly or after bouncing off the topside structure of the ship, which is usually so large and complex that it defies numerical treatments using rigorous CEM tools. However, the phased-array problem, although large in dimensions, cannot be treated via asymptotic techniques for most realistic arrays. The large aperture of the array is difficult to handle using ray methods because the topside scatterers are in the near field of the antenna; hence, the illumination impinging on the scatterers from the antenna is not a ray field. The usual approach is to break up the aperture of the antenna into pixels, each with a size that is small enough to satisfy the criterion that it radiates a ray field at the location of the scatterer. However, since the aperture size of the array can be large – e.g., on the order of $100\lambda \times 100\lambda$ – the number of such pixels becomes exorbitantly large for the ray optical

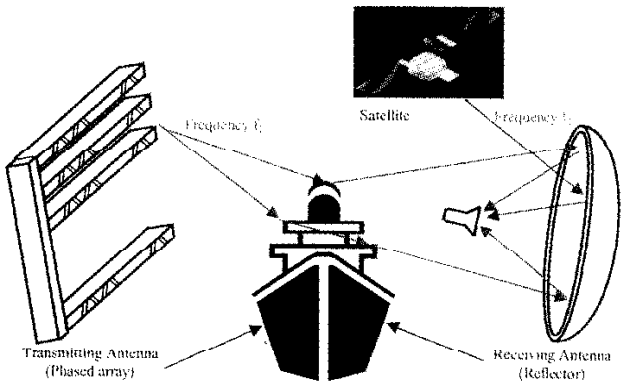

Figure 12. A coupling problem between a large phased-array antenna and a reflector antenna, operating in the topside environment.

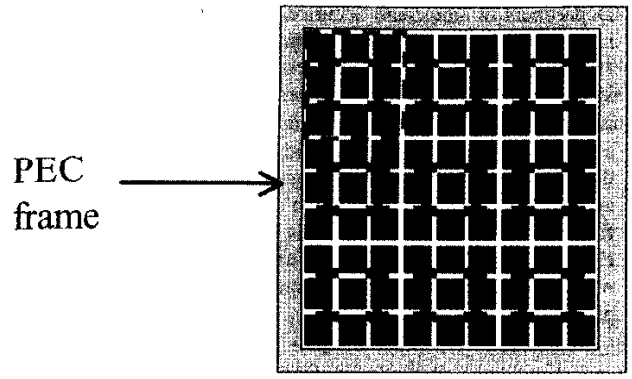

Figure 10. A top view of a microstrip-patch array covered by an FSS radome with cross-shaped elements.

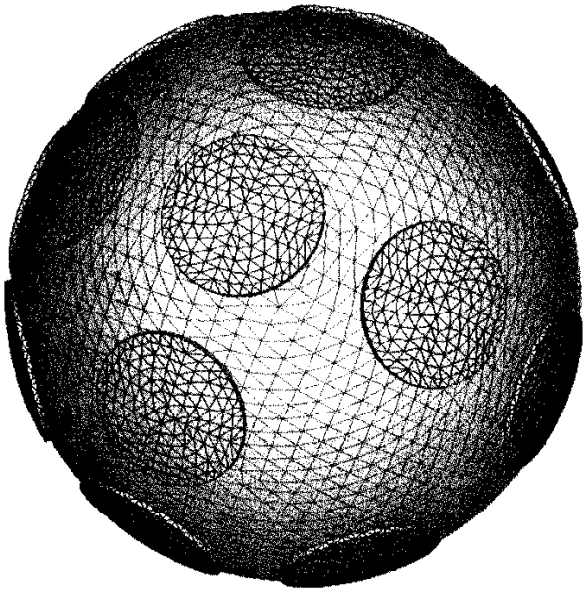

Figure 11. A conformal array of 13 circular patch antennas mounted on the surface of a dielectric sphere with a perfectly conducting core.

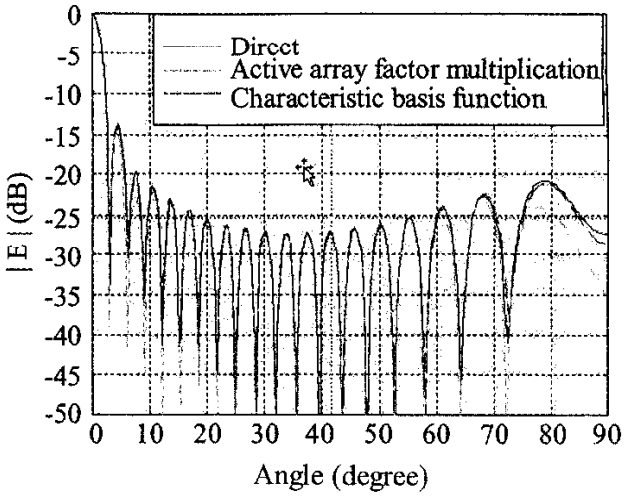

Figure 14. The E-plane far-field patterns of a 21 × 21 rectangular waveguide array.

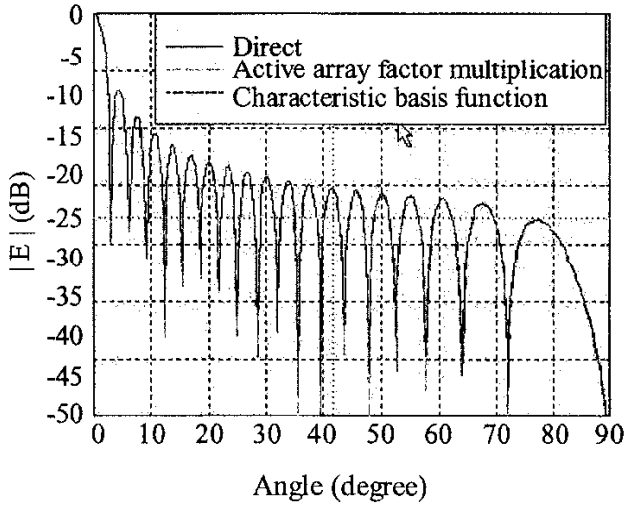

Figure 15. The H-plane far-field patterns of a 21 × 21 rectangular waveguide array.

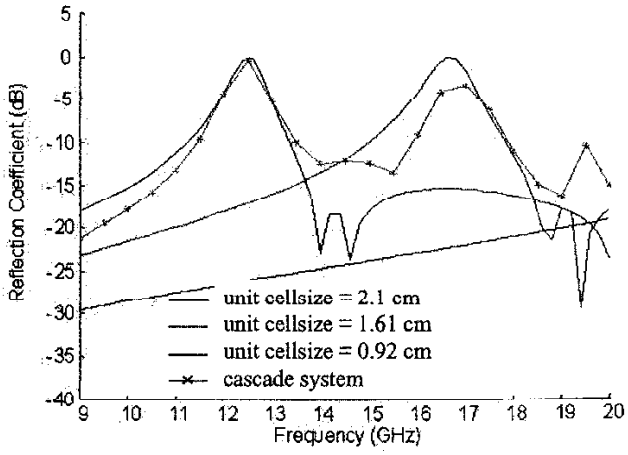

Figure 22. The reflection coefficient of the individual FSS screens and of the composite system.

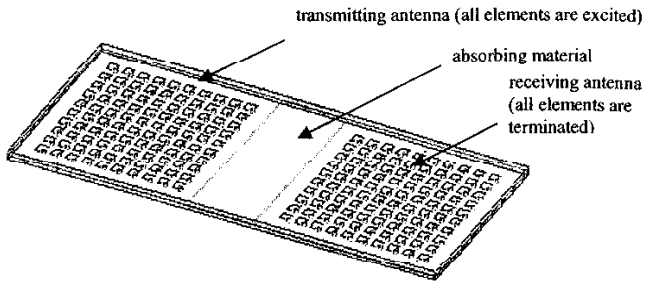

Figure 13. A problem of coupling between two array antennas with absorbing material inserted between them.

code to handle if this scheme is followed, and if the pixel size is on the order of $\lambda/10 \times \lambda/10$. An approach that reduces this number by several orders of magnitude is based on the use of equivalent sub-apertures that are much larger in size. However, such sub-apertures must first be constructed by processing the aperture fields using filtering techniques. These filtering techniques suppress the rapidly varying fields that contribute primarily to the evanescent fields, rather than to the radiating fields (a brief description of this approach may be found in [9]).

Even if one is able to satisfactorily resolve the problem of interfacing the array-antenna analysis codes with those for ray tracing, there still remains the difficult problem of determining the output of a receiver connected to the "victim" antenna, which may be another array, or a reflector. Interfacing the ray-optical codes with the rigorous codes that analyze these antennas (with large apertures and complex feed systems) operating in the receiving mode represents a very formidable challenge, indeed.

2.7 Near-Zone Coupling between Aperture Antennas

Another coupling problem of great interest pertains to antennas on complex structures. An example may be two aperture antennas (e.g., phased arrays sharing the same mast, or an airplane wing, for instance) with a separation distance that is not sufficiently large to allow the use of ray techniques. The presence of radar-absorbing materials between the antennas, often inserted to reduce the inter-aperture coupling between them, renders the problem even more difficult to handle. Thus, the near-field coupling problem between antennas sharing the same platform is even more challenging than the single-array problem (see Figure 13), not only because the combined size is larger, but also because the environment is more complex. Currently, there are several efforts underway for attacking this type of coupling problem, which presents a very formidable challenge, indeed.

2.8 EMI Problem Involving Electronic Systems Located Inside Buildings

As we well know, electronic systems such as computers are vulnerable to exposure to high-power electromagnetic waves. The security of these systems has become a major concern for several government agencies, exemplified by the "Special Technology Countermeasures and Defense Against Radio-Frequency Attack Program" of US NAVSEA, as well as by programs of the US Department of Homeland Security. The spectrum of the threat signal can be very wide, ranging from the megahertz to gigahertz range, and this makes the problem very large for realistic buildings. It is also evident that the interior environment of the building is very complex, since the computers and other electronic systems can be scattered at different locations inside the building, as can be the furniture and cabinets housing them. Perhaps the only realistic approach to attacking the problem of estimating the strength of the field coupled inside the building is to resort to a statistical method. However, it is often necessary to make many simulation runs from which the statistics can be extracted to develop such a statistical profile.

In common with several other problem geometries we have discussed above, this one also falls into the category that it is not amenable to attack via ray techniques, despite the fact that the problem dimensions we need to deal with are large compared to the wavelength. Multiple scattering from highly inhomogeneous objects precludes the use of ray methods, and we must resort to numerically rigorous techniques. Of these, the FDTD appears to be the most suited for the problem at hand, not only because it is highly parallelizable, but also because it can handle arbitrarily inhomogeneous structures. However, it should be realized that even with a distributed platform, the problem size can be much too large and unmanageable without the use of special techniques. One such technique has recently been developed, and some representative results based on this approach are presented in the next section.

3. Representative Results

The set of eight examples described in the last section by no means covers all the challenging CEM problems that we face today in the areas of antennas, scattering, and coupling (EMI/EMC). (Note: We have purposely omitted microwave circuit-simulation problems in this list.) Nevertheless, they do present a good cross section of practical, real-world problems that we face today in the process of designing systems for many communication and radar applications. Also, despite their diversity, the problems listed above share at least one common attribute: they all are big, complex, and very challenging. So, the next question – a logical one – that we ask is: What might be some of the viable approaches to solve them?

It would be too pretentious for this author to claim to have the answers. However, having been involved in a number of recent projects in which problems like these were encountered by the author, it may be useful to share with the readers two techniques that are being specifically developed for addressing the above category of problems. We are referring to the Windowed Plane Wave Spectrum (WPWS) technique and the Characteristic Basis Function Method (CBFM), introduced recently by the author and his colleagues in a number of publications [1-4, 15-20]. This write-up is thus basically a summary of the recent techniques developed at the EMC Laboratory at Penn State and at RM Associates, in the course of working on a number of projects of interest to the US Department of Defense and its contractors.

Of course, there are a number of other researchers (for instance, the authors of [7-10, 21-30]) who have also addressed problems of this type, and the list of contributors is by no means comprehensive. Once again, reviewing the other approaches is beyond the scope of this paper, and the interested reader is strongly encouraged to refer to these excellent publications on the subject for further details.

Returning then to the CBFM, a detailed discussion of this method is also beyond the scope of this paper, and the reader is again referred to the relevant publications on the subject. We will instead limit ourselves to the presentation of some representative results for a number of the challenging problems described in the last section.

3.1 Large Array Problem

Figures 14 and 15 show the results for the E- and H-plane patterns of a 21 by 21 waveguide array, computed directly as well as via the CBFM. The latter begins by generating the solution for a number of local subdomains – including the center, edges, and corners of the array – and then combines them suitably to synthesize the solution to the entire problem. As might be expected, the direct solution to this problem is very CPU intensive, and requires far more time (and memory) than does the CBFM. Perhaps even more important is the fact that it takes little additional time and memory to solve the problem of an 81 × 81 array, which is altogether too large to be handled directly, since it requires more than 3×10^9 unknowns for accurate simulation using the FDTD method. The CBFM results for the 81 × 81 array problem are presented in Figures 16 and 17, just to demonstrate that this (and even much larger) size problems can be handled with the CBFM without running into any difficulties or roadblocks in terms of CPU time or memory usage.

3.2 Truncated FSS Radome Problem

As mentioned earlier, using the Windowed Plane Wave Spectrum (WPWS) approach combined with MoM analysis is a relatively easy way to construct the solution to a large, truncated FSS problem. In Figure 18 we present the results for a 25 × 25 FSS screen of rectangular patches (the element shape can be arbitrary, as long as it is thin). The scattered far field of this finite FSS is plotted in Figure 18. Once again, the size of the FSS matters little when the Windowed Plane Wave Spectrum approach is used, and this is a significant advantage of the method.

It is interesting to mention that the same problem, solved by using the Fast Multipole Method (FMM) for the simpler case of a free-standing FSS (the FMM cannot conveniently handle the dielectric-loaded case, though it can analyze arbitrarily-shaped three-dimensional PEC objects, which this version of the Windowed Plane Wave Spectrum cannot) takes considerably more time and memory than does the Windowed Plane Wave Spectrum approach (see Table 1).

When the FSS is thick or inhomogeneous, we can employ the CBFM in conjunction with the FDTD. This can be done in much the same way we did when we solved the large array problem, viz., by first solving sub-problems associated with the different zones and then synthesizing the final solution from these component solutions. It should be mentioned that the illumination for these sub-problems is also windowed, to suppress the spurious edge effects that appear when the incident plane wave is suddenly truncated to make it nonzero only inside the zone it is illuminating.

3.3 Non-Commensurate FSS Analysis

A brute-force approach to analyzing a cascaded FSS composite with constituent screens that have non-commensurate peri-

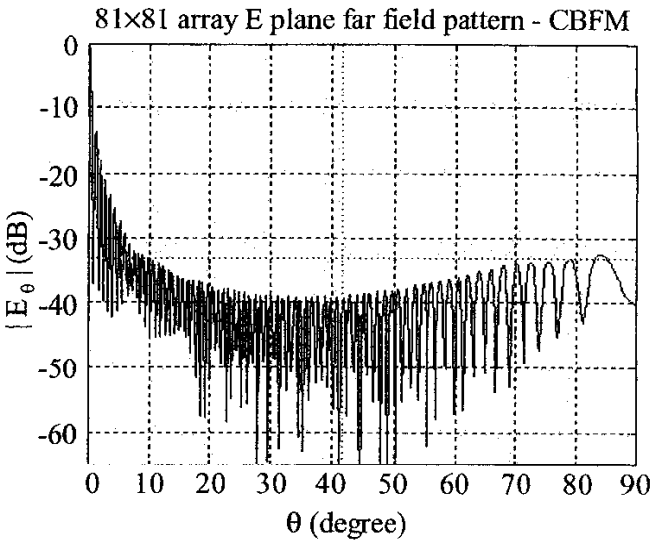

Figure 16. The E-plane far-field pattern of an 81 × 81 rectangular waveguide array.

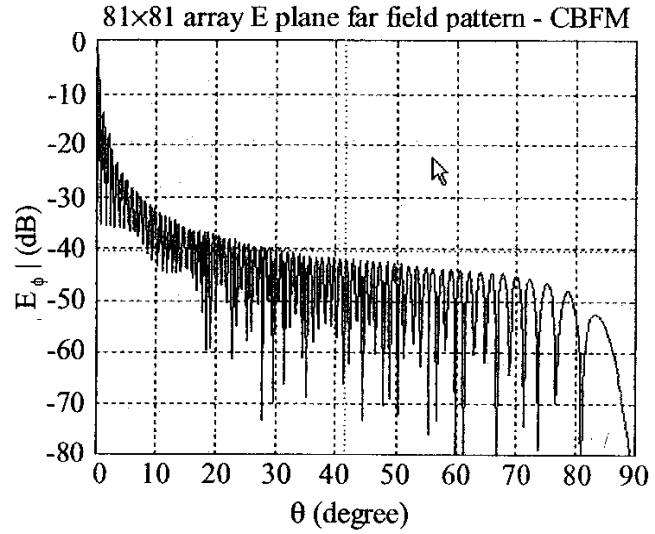

Figure 17. The H-plane far field pattern of 81 × 81 rectangular waveguide array.

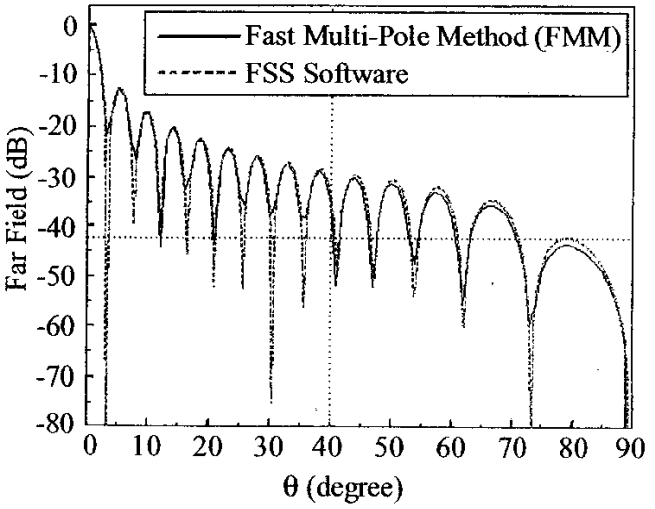

Figure 18. The scattered far field from a finite FSS, illuminated by a normally incident plane wave.

Table 1. Performance comparison of the MLFMM and the present approach for a finite free-standing FSS problem.

	MLFMM	Present Approach
Memory	1087 MB	19 MB
CPU Time	25212 s	689 s
Machine Configuration	IBM RS6000	PC 662 MHz

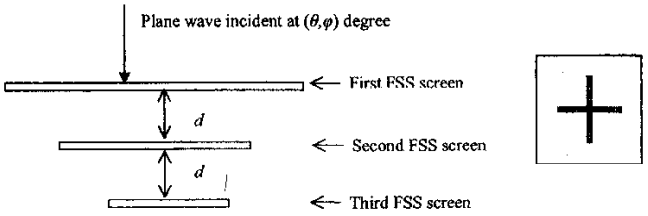

Figure 19. A non-commensurate composite structure consisting of three stacked subsystems (side view).

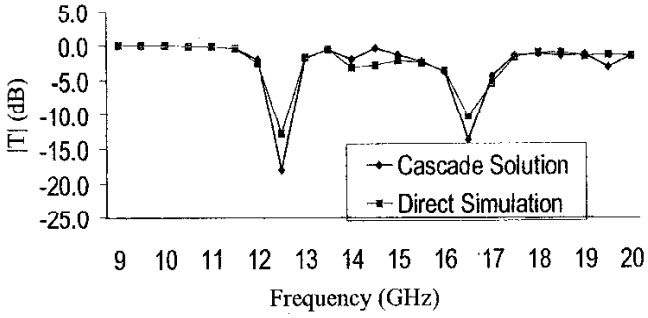

Figure 20. A comparison of the magnitudes of the transmission coefficient (TE-TE polarization) of the composite of Figure 19 at normal incidence, for the direct simulation and the cascade solution.

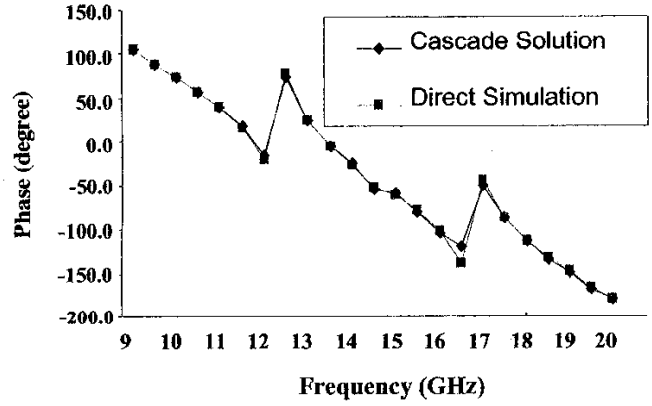

Figure 21. A comparison of the phases of the transmission coefficient (TE-TE polarization) of the composite of Figure 19 at normal incidence, for the direct simulation and the cascade solution.

odicities is not really practical for real-world problems. This is because one must simultaneously solve for the current distributions on multiple screens that are typically many wavelengths in size. Instead, the method introduced in [12, 31] defines a global system by selecting one of these screens as the dominant screen, on the basis of the closeness of its resonant frequency to the operating frequency. Following this, a systematic approach is used to determine the number of unit cells of the different screens that are embraced by the global period within a certain tolerance limit. Finally, global scattering matrices are constructed in a computationally efficient manner, and are subsequently cascaded to generate the S parameter of the composite. Figures 20 and 21 present the results for a test system comprised of three FSSs with elements that are crossed dipoles (note: they could be of arbitrary shape). The unit-cell dimensions of the three screens were 2.1 cm × 2.1 cm, 1.61 cm × 1.61 cm, and 0.92 cm × 0.92 cm, and the spacing, d, was 0.75 cm. The frequency range of interest was 9 GHz to 20 GHz (Figure 19).

The magnitude and the phase of the transmission coefficients are plotted in Figures 20 and 21 for $\theta = 0°$ and $\phi = 0°$, where the results of direct computation (approximate) are also shown. We note that the agreement is good, and we point out that the direct approach was several orders of magnitude more expensive in terms of CPU time than the approach we have described above. Also, it was necessary to sacrifice the accuracy somewhat in the direct approach in order to be able to handle the problem at all.

The individual transmission and reflection coefficients of the screens are plotted together with those of the composite for comparison in Figures 22 and 23. The differences in the resonant characteristics of the individual screens are quite apparent from the above plots.

3.4 Array Covered by an FSS Radome

As mentioned in the previous section, a perturbation approach can be used to handle this problem for weak-to-moderate interaction between the array and the radome, and this approach is quite efficient for handling large systems, even when the periodicities of the FSS and the array are non-commensurate. We start with the aperture field of the array, which may be derived by using any available method, including the CBFM. We can then take this aperture field – assuming that it is not substantially altered by the presence of the radome – and express on in a spectrum of plane waves. We can then treat each of these as discussed in the previous subsection when we dealt with a single incident plane wave, and proceed to synthesize the solution for the more general illumination produced by the phased array. A sample result for a 9 × 9 microstrip patch array covered by an FSS radome (see Figure 5) is presented in Figure 24. We remark that to solve this composite problem directly would be extremely difficult, if not impossible, with usual computer resources for realistic arrays that are much larger; however, they present little difficulty when approached with the CBFM.

Next, we briefly touch on a case example where the array and the radome are tightly coupled and, hence, the perturbation approach just described above is no longer viable. However, the

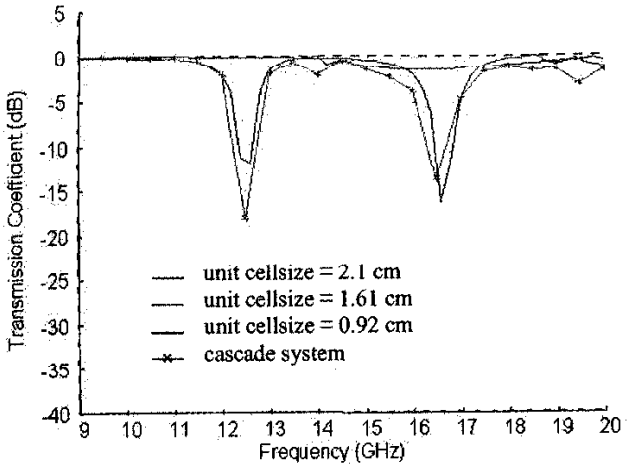

Figure 23. The transmission coefficients of the individual FSS screens and of the composite system.

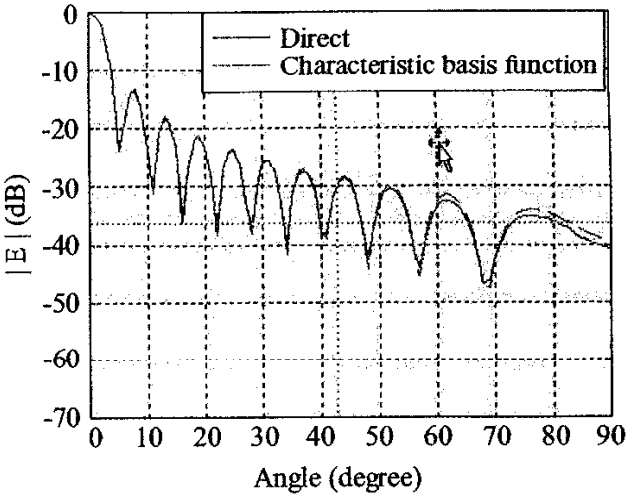

Figure 27. The H-plane far-field pattern of a 7 × 7 macro-unit-cell array (441 patches).

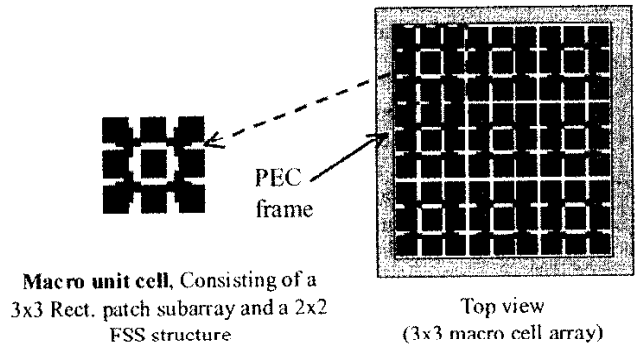

Figure 25. An application of the CBFM to a phased array of microstrip patches covered by a cross-shaped FSS radome (note that the periods are not commensurate).

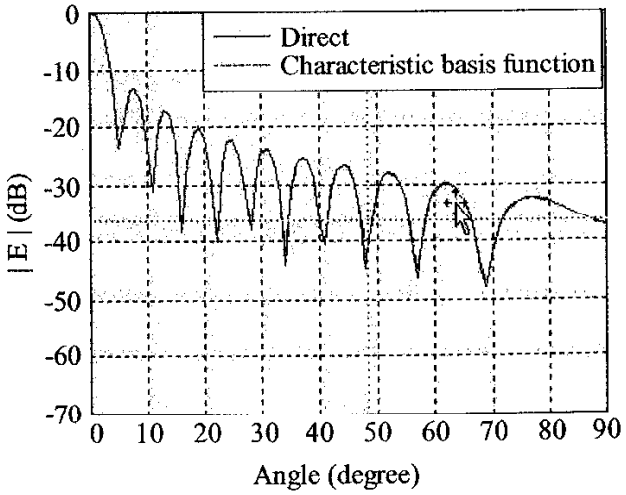

Figure 26. The E-plane far-field pattern of a 7 × 7 macro-unit-cell array (441 patches).

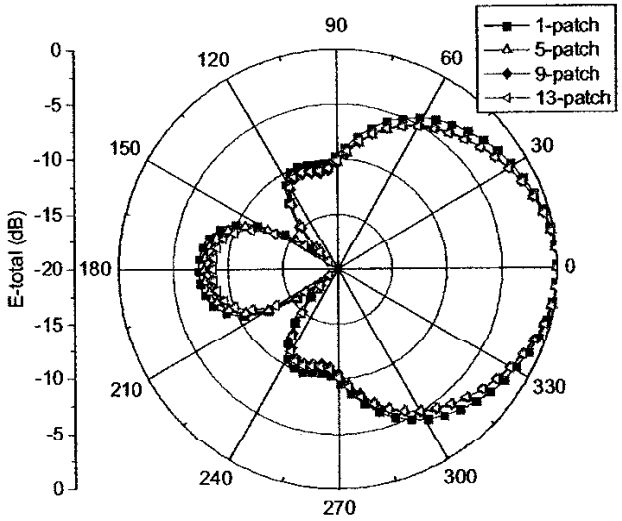

Figure 28. The normalized far-field patterns in the *x-z* plane, $\phi = 0°$.

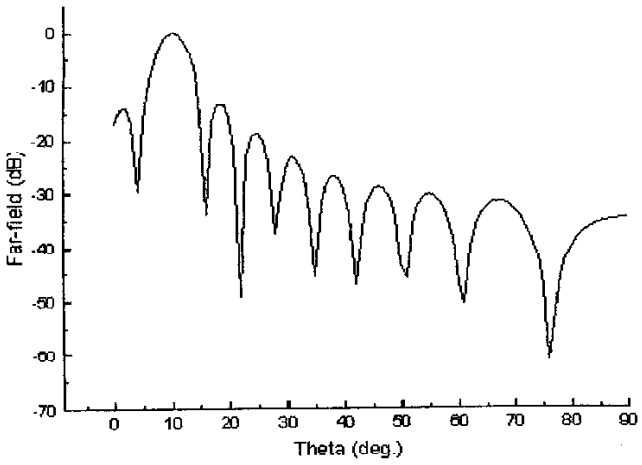

Figure 24. The radiated far field of a microstrip array with a finite FSS at 15 GHz.

CBFM still can be used to handle this problem [31], again by localizing the partial solutions in different subdomains and then synthesizing the solution to the original problem in the same manner as before (see Figure 25).

Figures 26 and 27 show the result for an array-radome composite, comprised of a 21 × 21 array and a 14 × 14 FSS radome. A comparison of the CBFM results with the direct solution for this size of problem (which is still manageable but costs considerably more when solved directly) is also presented in the same figure. The CBFM can, of course, handle much larger problems with little additional computational burden.

3.5 Conformal Array Example

In common with the planar array, the conformal version of the array, shown in Figure 11, is also treatable with the CBFM, perhaps even more so than the planar problem. This is because the coupling to adjacent elements from an excited element falls off even more rapidly than it does in the planar case; hence, the problem is localized relatively easily.

We demonstrate this by presenting, in Figures 28 and 29, the results for the far-field pattern of the array in Figure 11 when only one patch was excited and the number of elements was progressively increased from one to 13 (see [33]). One could therefore generate localized solutions once again, and synthesize the solution to the total problem in a manner similar to what was done for the planar array. A comparison of the synthesized result with the direct calculation is shown in Figure 30.

3.6 EMI/EMC Problem Between Antennas Operating in the Topside Environment

We now present some results for the equivalent sub-aperture approach, mentioned in Section 2.6. Results for a 90 × 90 phased array are given in Figures 31 and 32 to show how well this approach reproduces the pattern of the entire aperture. The subaperture size was 2.17 in × 2.17 in, considerably larger than the pixel size used in the original FDTD simulation. Comparisons between the original and sub-aperture far-field patterns are seen to be quite good, and the reduction of the computational burden realized via the use of the sub-aperture approach was substantial, rendering the problem viable. The CPU time to carry out the coupling calculations between two large antennas operating in a realistic shipboard environment using the ray-tracing approach could easily be more than one year per frequency point if the original $\lambda/10 \times \lambda/10$ pixels were used.

In Figure 33 we show a flowchart of the steps we followed to determine the output of a receiver connected to the feed of a reflector antenna that was simultaneously receiving the desired signal at a frequency of 3.0 GHz, together with an interfering signal at 6.5 GHz. The receiver calculations, shown in Figure 34, were made by using the *Microwave Office* software, available from Applied Wave Research.

We implicitly assumed that the fields radiated by the phased array made their way to the reflector after undergoing multiple scattering from the topside environment, and that a ray-tracing code provided us the fields thus excited in the aperture of the reflector. To determine the signal coupled into the feed of the

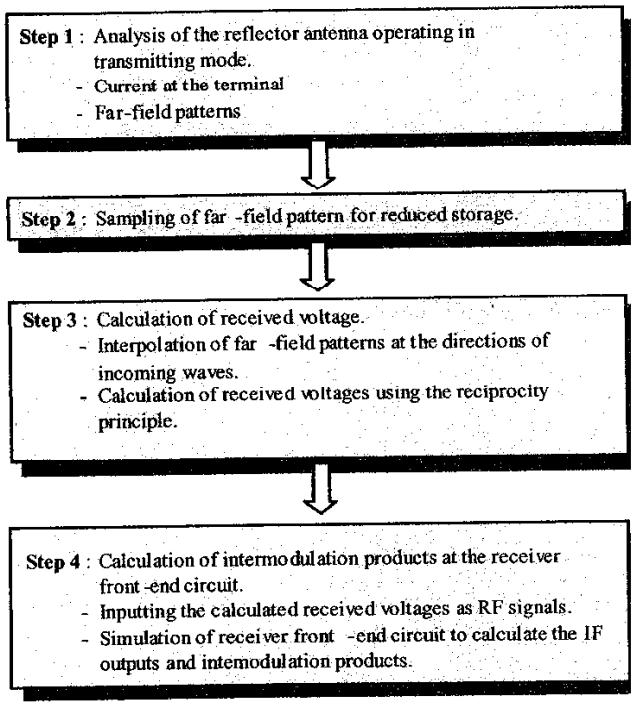

Figure 33. The steps used to calculate the output of a receiver connected to the feed of a reflector antenna.

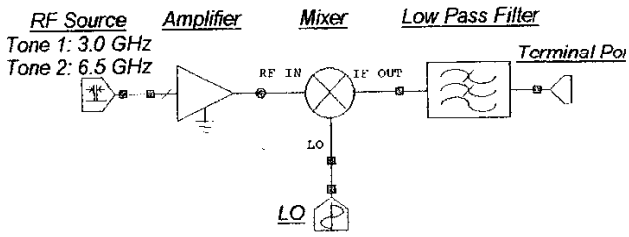

Figure 34. A schematic diagram of the receiver front-end circuit (modeled in *Microwave Office*).

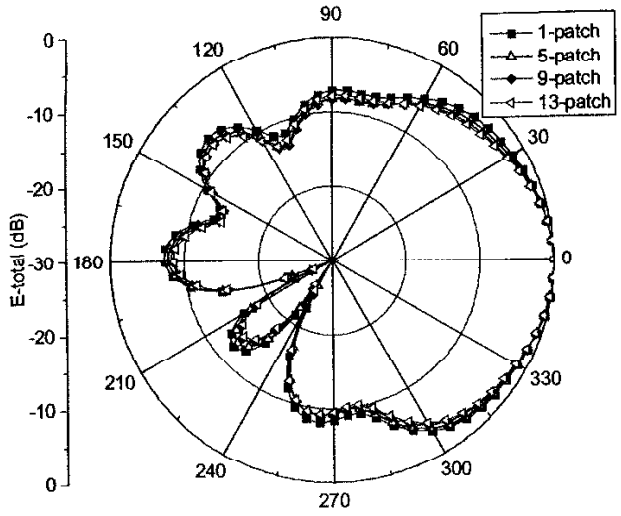

Figure 29. The normalized far-field patterns in the y-z plane, $\phi = 90°$.

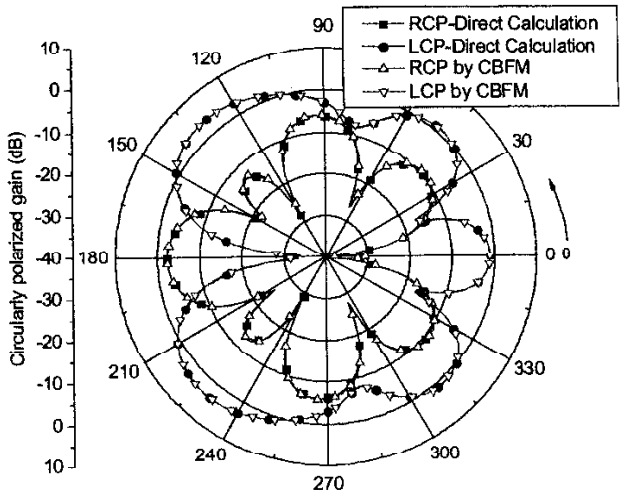

Figure 30. A comparison of the far-field pattern synthesized with the CBFM and those patterns obtained by direct calculation.

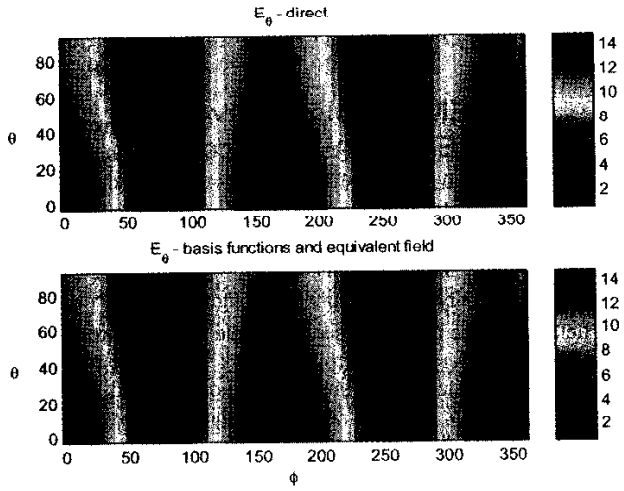

Figure 31. A comparison between the θ components of the far-field pattern for the original (direct) and equivalent aperture fields.

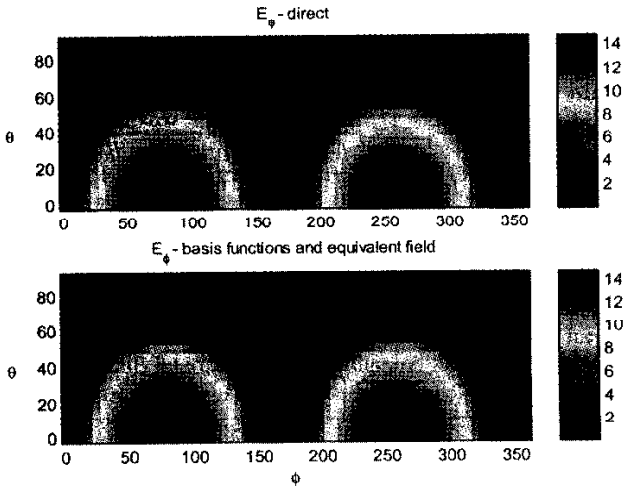

Figure 32. A comparison between the ϕ components of the far field pattern for the original (direct) and equivalent aperture fields.

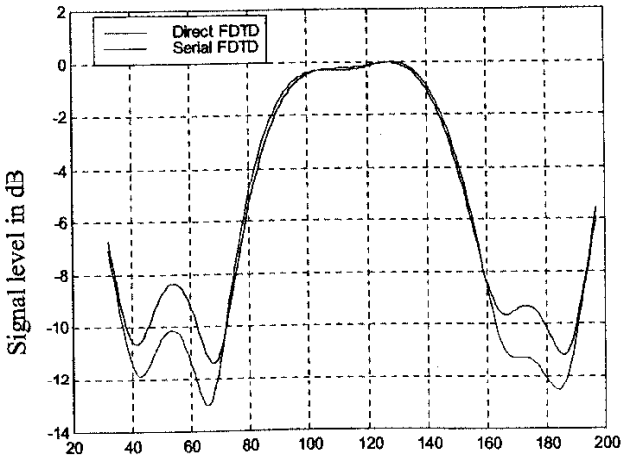

Figure 37. The magnitude of the field distribution using three reflections.

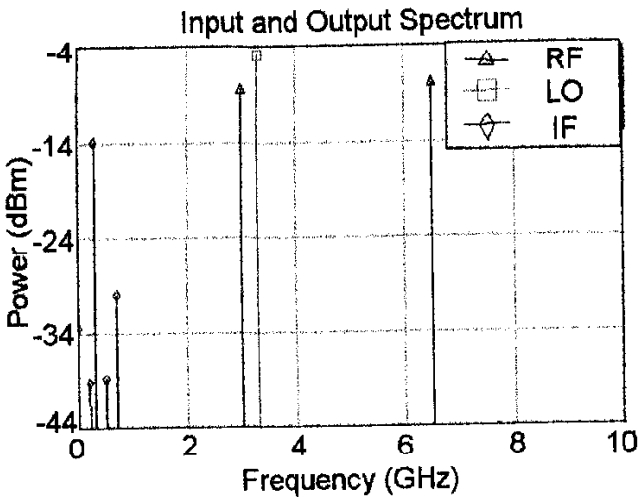

Figure 35a. The output spectra after the preamp in the receiver front-end circuit shown in Figure 34.

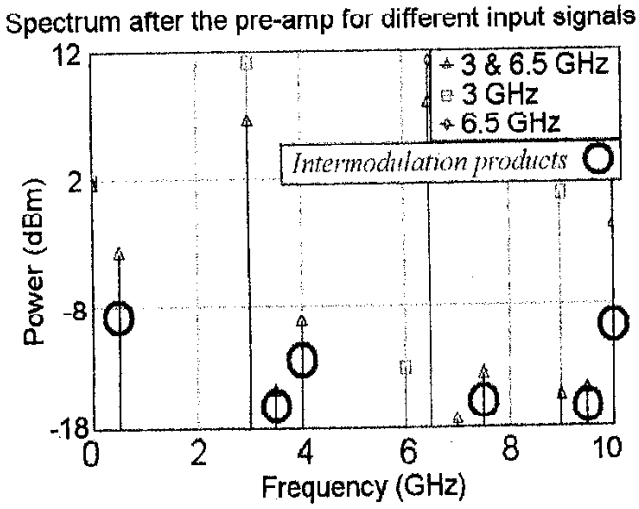

Figure 35b. The input and output spectrum for the receiver front-end circuit shown in Figure 34.

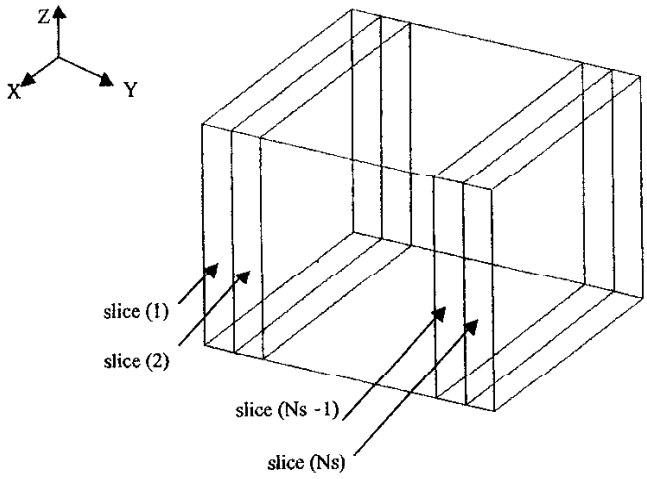

Figure 36. The domain decomposition of a structure into small slices for serial computations.

reflector, we used an approach based on the reciprocity principle, and computed the field in the aperture of the reflector operating in the transmitting mode when it was excited by a unit voltage source. Next, we took a scalar product of this transmitted aperture field with the field received from the array (also in the same reflector aperture) to obtain the desired coupled voltage. Finally, we estimated the level of interference and intermodulation (IM) products generated in the receiver by using an electronics code such as *Microwave Office*. A schematic of the receiver and its output spectra are presented in Figure 35 for two-tone signals (3.0 GHz and 6.5 GHz)

3.7 Near-Zone Coupling

As mentioned earlier, the near-zone coupling problem, shown in Figure 13, must be addressed by using numerically rigorous techniques, and we might view it as an extension of a single aperture to which we had applied the CBFM. We omit further details here, and simply mention that the example in Figure 13 is a relatively small problem that can still be analyzed directly, while the CBFM is applicable to much larger problems that are beyond the scope of direct methods

3.8 EMI Problems Involving Electronic Devices

To illustrate the application of CBFM to the problem of coupling into a building, we divided the building into several slices, as explained in [34] and shown in Figure 36. We then solved the problem sequentially from regions 1 through N_s using the interface fields from the preceding section as the virtual source for the following one. The reflection from the back wall of the room was accounted for by running the simulation another round but in the backward direction, dealing only with the backward-traveling excitations. Figure 37 shows a comparison between the results obtained by using this version of the CBFM and those obtained directly, and they are found to compare well in the region of interest (the high-field region). By using a parallel version of the code in each of the regions and combining the solutions with the serial approach, very large problems of this type can be solved with only moderate computer resources. This is in general true not only for the application of the CBFM for this problem, but also to others we have discussed earlier.

4. Conclusion

In this paper we have attempted to provide a short glimpse of some of the challenging antenna and scattering problems faced today by the designers of electromagnetic systems, including antennas on complex platforms.

The paper has also provided a quick glance at a recently-developed approach CBFM) for addressing these problems in a numerically efficient manner. The method was developed at the EMC Laboratory of Penn State and at RM Associates, with colleagues at the Universities of Pisa (Profs. Agostino Monorchio and Giuliano Manara), Middle Eastern Technical University (Prof Mustafa Kuzuoglu), and the City University of Hong Kong (Profs Chi Chan and L. Tsang). It is hoped that this brief write-up will

spark an interest in the antennas and propagation community, and will inspire its members to tackle the group of challenging problems identified in this paper with their own arsenal of innovative methods.

5. Acknowledgement

The author gratefully acknowledges the help of Kai Du, N. Farahat, N. T. Huang, Lai-Ching Ma, V. V. S. Prakash, Hany Abdel-Raouf, Tao Su, and Wenhua Yu, all affiliated with of the EMC Lab at Penn State, without whose help and extensive contributions to this text this article could not have been written. Thanks are also due to Prof. Y. Antar for inviting the author on behalf of the *Magazine* to submit this paper that might be of interest to the antennas and propagation community.

6. References

1. V. V. S. Prakash and R. Mittra, "Characteristic Basis Function Method: A New Technique for Efficient Solution of Method of Moments Matrix Equations," *Microwave & Optical Technology Letters*, **36**, 2, January 2003, pp. 95-100.

2. R. Mittra and V. V. S. Prakash, "The Characteristic Basis Function Method: A New Technique for Fast Solution of Radar Scattering Problem," *Computer Modeling in Engineering & Sciences*, **5**, 5, 2004, pp. 435-442 .

3. R. Mittra, "Solution of Large array and Radome Problems using the Characteristic Basis Function Approach," USNC/URSI National Radio Science Meeting, Columbus, Ohio, June 2003.

4. R. Mittra, "A Proposed New Paradigm for Solving Scattering Problems Involving Electrically Large Objects using the Characteristic Basis Functions Method," *Proceedings of the International Conference on Electromagnetics in Advanced Applications (ICEAA) 2003*, Turin, Italy, September 2003, pp. 621-623.

5. R. Mittra, V. V. S. Prakash, and T. Q. Ho, "A Novel Approach to Analyzing Truncated Frequency Selective Surface Radomes Operating in the Proximity of Array Antennas," Electromagnetic Code Consortium (EMCC) Annual Meeting, Kawai, HI, May, 2001.

6. V. V. S. Prakash, N. T. Huang, and R. Mittra, "Accurate Analysis of Interaction Between Microwave Antennas and Frequency Selective Surface (FSS) Radomes," *Proceedings of the Twelfth International Conference on Antennas and Propagation (ICAP)*, University of Exeter, UK, **1**, April 2003, pp. 401-404.

7. R. W. Kindt and J. L. Volakis, "Finite Array Analysis Using a Multi-Dimensional, Multi-Cell Hybrid Array Decomposition-Fast Multipole Method," *Proceedings of the International Conference on Electromagnetics in Advanced Applications (ICEAA) 2003*, Turin, Italy, September 2003, pp. 317-320.

8. F. Capolino, S. Maci, M. Sabbadini, L. Felsen "Large Phased Array on Complex Platform," International Conference on Electromagnetics in Advanced Applications," *Proceedings of the International Conference on Electromagnetics in Advanced Applications (ICEAA)*, Torino, Italy, September 10-14, 2001.

9. P. Pirinoli, F. Vipiana, L. Matekovits and G. Vecchi, "Multiscale Analysis of Large Complex Arrays," *Proceedings of the International Conference on Electromagnetics in Advanced Applications (ICEAA) 2003*, Turin, Italy, September 2003, pp. 605-608.

10. A. Neto, S. Maci, G. Vecchi, M. Sabbadini, "A Truncated Floquet Wave Diffraction Method for the Full Wave Analysis of Large Phased Arrays. Part 11: Generalisation to the 3D Case," *IEEE Transactions on Antennas and Propagation*, **48**, 3, April 2000, pp. 601-611.

11. T. K. Wu, *Frequency Selective Surfaces and Grid Array*, New York, Wiley, 1995.

12. J. F. Ma, R. Mittra and N. T. Huang, "Analysis of FSS Composites Comprising of Multiple FSS Screens of Unequal Periodicity," IEEE International Symposium on Antennas and Propagation *Digest*, Columbus, Ohio, June 2003, **2**, pp. 801-804.

13. Alan F. Kay, "Electrical Design of Metal Space Frame Radomes," *IEEE Transactions on Antennas and Propagation*, **AP-11**, 10, October, 1963, pp. 188-202.

14. W. V. T. Rusch, Jorgen Appel-Hansen, Charles A. Klein, and Raj Mittra, "Forward Scattering from Square Cylinders in the Resonance Region with Application to Aperture Blockage," *IEEE Transactions on Antennas and Propagation*, **AP-24**, 2, March 1976, pp. 182-189.

15. T. Su, L. Ma, N. Farahat, and R. Mittra, "Modeling of a Large Slotted Waveguide Phased Array using the FDTD and Characteristic Basis Function (CBF) Approaches," USNC/URSI National Radio Science Meeting, Columbus, OH, June 2003.

16. V. V. S. Prakash, "RCS computation over a Frequency Band using the Characteristic Basis and Model Order Reduction Method," IEEE International Symposium on Antennas and Propagation *Digest*, Columbus, Ohio, June 2003, **1**, pp. 89-92.

17. R. Mittra and V. V. S. Prakash, "The Characteristic Basis Function Method (CBFM) – An Alternative to FMM for a Class of Antenna and Scattering Problems," USNC/URSI National Radio Science Meeting, Columbus, Ohio, June 2003.

18. Kai Fai Chan, King Wai Lam, Chi Hou Chan, and Raj Mittra, "Fast Computational Techniques for the Analysis of Microstrip Reflectarrays," *IEEE Transactions on Antennas and Propagation* (to appear).

19. M. Kuzuoglu and Raj Mittra, "Fast Solution of Electromagnetic Boundary Value Problems by the Characteristic Basis Functions/FEM Approach," IEEE International Symposium on Antennas and Propagation, Columbus, Ohio, June 2003, **2**, pp. 1071-75.

20. Y. F. Sun, C. H. Chan, R. Mittra, and L. Tsang, "Characteristic Basis Function Method for Solving Large Problems Arising in Dense Medium Scattering," IEEE International Symposium on Antennas and Propagation *Digest*, 2003, June 22-27, 2003, **2**, pp. 1068-1071.

21. A. Cucini and S. Maci, "Surface and Leaky Wave Excitation in Large Finite Periodic Microstrip Arrays," *Proceedings of the International Conference on Electromagnetics in Advanced Applications (ICEAA) 2003*, Turin, Italy, September 2003, pp. 341-344.

22. B. Fasenfest, F. Capolino, D. R. Wilton, D. R. Jackson, and N. Champagne, "General MoM Solutions for Large Arrays," *Proceedings of the International Conference on Electromagnetics in Advanced Applications (ICEAA) 2003*, Turin, Italy, September 2003.

23. A. G. Tijhuis, M. C. van Beurden, and E. Korkmaz, "Modeling Electromagnetic Fields in Large, Finite Structures Using Iterative Techniques and the Equivalence Principle," *Proceedings of the International Conference on Electromagnetics in Advanced Applications (ICEAA) 2003*, Turin, Italy, September 2003, pp. 625-628.

24. R. W. Kindt, K. Sertel, E. Topsakal, and J. L. Volakis, "Array Decomposition Method for the Accurate Analysis of Finite Arrays," *IEEE Transactions on Antennas and Propagation*, **51**, 6, June 2003, pp. 1364-1372 .

25. R. Kindt and J. L. Volakis, "A Multi-Cell Array Decomposition Approach to Composite Finite Array Analysis," IEEE International Symposium on Antennas and Propagation *Digest*, Columbus, Ohio, June 2003, **1**, pp. 15-18.

26. L. Matekovits, G. Vecchi, G. L. Dassano, and M. Orefice, "Synthetic Function Analysis of Large Printed Structures: the Solution Space Sampling Approach," IEEE International Symposium on Antennas and Propagation *Digest*, Boston, Massachusetts, USA, 8-13 July 2001, pp. 568-571

27. P. Pirinoli, G. Vecchi, L. Matekovits, "Multiresolution Analysis of Printed Antennas and Circuits: A Dual-Isoscalar Approach," *IEEE Transactions on Antennas and Propagation*, **AP-49**, 6, June 2001, pp. 858-874.

28. P. Pirinoli and G. Vecchi, "An Adaptive Multiresolution Approach to the Simulation of Planar Structures," *IEEE Microwave and Wireless Components Letters*, **12**, February 2002, pp. 45-47.

29. A. G. Tijhuis, M. C. van Beurden and A. P. M. Zwamborn, "Iterative Solution of Field Problems with a Varying Physical Parameter," *Elektrik*, **10**, 2, 2002, pp.163-183.

30. S. Maci, G. Vecchi, A. Freni, "Matrix Compression and Supercompression Techniques for Large Arrays," IEEE International Symposium on Antennas and Propagation *Digest*, Ohio, June, 2003, pp. 1064-1067.

31. R. Mittra and N. T. Huang, "Numerically Efficient Analysis of Large Array and FSS Radome Composites with Dissimilar Periodicities," *Proceedings of the International Conference on Electromagnetics in Advanced Applications (ICEAA) 2003*, Turin, Italy, September 2003, pp. 313-316.

32. R. Mittra, "Characteristic Basis Function Method for Analyzing Large Arrays Covered by Frequency Selective Radomes with Dissimilar Periods," 2003 EM Code Consortium Annual Meeting, May 2003.

33. K. Du, N. Farahat, H. Abd El-Raouf, T. Su, W. H. Yu, and R. Mittra, "Simulation of Circular Patch Antenna on a Sphere Using the Conformal Finite Difference Time Domain (CFDTD) Algorithm," IEEE International Symposium on Antennas and Propagation *Digest*, Columbus, Ohio, June 2003, Vol. 2, pp. 988-991.

34. H. E. Abdel-Raouf and R. Mittra, "A Novel Longitudinal-section FDTD algorithm for Simulating Large-size Electromagnetic Compatibility and Interference (EMC/EMI) Problems," USNC/URSI National Radio Science Meeting, Columbus, OH, June 2003.

Introducing the Feature Article Author

Raj Mittra is a Professor in the Electrical Engineering Department of the Pennsylvania State University. He is also the Director of the Electromagnetic Communication Laboratory which is affiliated with the Communication and Space Science Laboratory of the Electrical Engineering department. Prior to joining Penn State, he was a Professor in Electrical and Computer Engineering at the University of Illinois in Urbana Champaign. He is a Life Fellow of the IEEE, a Past President of AP-S, and he has served as the Editor of the *IEEE Transactions on Antennas and Propagation*. He won the Guggenheim Fellowship Award in 1965, the IEEE Centennial Medal in 1984, the IEEE Millennium Medal in 2000, the AP-S Distinguished Achievement Award in 2002, and the AP-S Chen-To Tai Distinguished Educator Award in 2004. He has been a Visiting Professor at Oxford University, Oxford, England, and at the Technical University of Denmark, Lyngby, Denmark. He has over 700 publications to his credit, as well as more than 30 books or book chapters on electromagnetics, antennas, microwaves and electronic packaging. He has supervised the completion of over 85 PhD dissertations, an equal number of MS theses, and has mentored over 50 postdocs.

Raj is the President of RM Associates, which is a consulting organization that provides services to industrial and government organizations, both in the US and abroad.